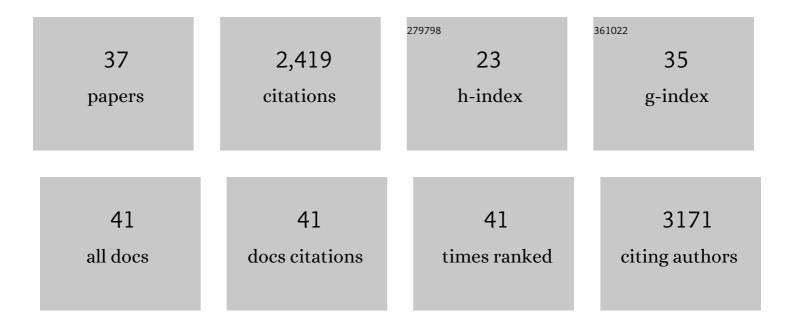
Weiqing Zheng

List of Publications by Year in descending order

Source: https://exaly.com/author-pdf/408894/publications.pdf Version: 2024-02-01



#	Article	IF	CITATIONS
1	Molecular structure, morphology and growth mechanisms and rates of 5-hydroxymethyl furfural (HMF) derived humins. Green Chemistry, 2016, 18, 1983-1993.	9.0	276
2	Production of Dimethylfuran from Hydroxymethylfurfural through Catalytic Transfer Hydrogenation with Ruthenium Supported on Carbon. ChemSusChem, 2013, 6, 1158-1162.	6.8	247
3	Experimental and Theoretical Investigation of Molybdenum Carbide and Nitride as Catalysts for Ammonia Decomposition. Journal of the American Chemical Society, 2013, 135, 3458-3464.	13.7	216
4	Individual Feâ^'Co Alloy Nanoparticles on Carbon Nanotubes: Structural and Catalytic Properties. Nano Letters, 2008, 8, 2738-2743.	9.1	200
5	Effects of CeO2 addition on Ni/Al2O3 catalysts for the reaction of ammonia decomposition to hydrogen. Applied Catalysis B: Environmental, 2008, 80, 98-105.	20.2	169
6	The Role of Ru and RuO ₂ in the Catalytic Transfer Hydrogenation of 5â€Hydroxymethylfurfural for the Production of 2,5â€Dimethylfuran. ChemCatChem, 2014, 6, 848-856.	3.7	136
7	Vapor phase hydrodeoxygenation of furfural to 2-methylfuran on molybdenum carbide catalysts. Catalysis Science and Technology, 2014, 4, 2340.	4.1	132
8	C–O bond activation using ultralow loading of noble metal catalysts on moderately reducible oxides. Nature Catalysis, 2020, 3, 446-453.	34.4	131
9	Polyethylene Hydrogenolysis at Mild Conditions over Ruthenium on Tungstated Zirconia. Jacs Au, 2021, 1, 1422-1434.	7.9	95
10	NH3 Decomposition Kinetics on Supported Ru Clusters: Morphology and Particle Size Effect. Catalysis Letters, 2007, 119, 311-318.	2.6	94
11	Structure–Function Correlations for Ru/CNT in the Catalytic Decomposition of Ammonia. ChemSusChem, 2010, 3, 226-230.	6.8	82
12	Solventless C–C Coupling of Low Carbon Furanics to High Carbon Fuel Precursors Using an Improved Graphene Oxide Carbocatalyst. ACS Catalysis, 2017, 7, 3905-3915.	11.2	72
13	Selective Hydrodeoxygenation of Vegetable Oils and Waste Cooking Oils to Green Diesel Using a Silica‣upported Ir–ReO _{<i>x</i>} Bimetallic Catalyst. ChemSusChem, 2018, 11, 1446-1454.	6.8	66
14	Cellulose Hydrolysis in Acidified LiBr Molten Salt Hydrate Media. Industrial & Engineering Chemistry Research, 2015, 54, 5226-5236.	3.7	63
15	Catalytic Hydrodeoxygenation of High Carbon Furylmethanes to Renewable Jetâ€fuel Ranged Alkanes over a Rheniumâ€Modified Iridium Catalyst. ChemSusChem, 2017, 10, 3225-3234.	6.8	54
16	Durable and self-hydrating tungsten carbide-based composite polymer electrolyte membrane fuel cells. Nature Communications, 2017, 8, 418.	12.8	42
17	Molybdenum Oxide-Modified Iridium Catalysts for Selective Production of Renewable Oils for Jet and Diesel Fuels and Lubricants. ACS Catalysis, 2019, 9, 7679-7689.	11.2	39
18	Nonâ€oxidative Coupling of Methane to Ethylene Using Mo ₂ C/[B]ZSMâ€5. ChemPhysChem, 2018, 19, 504-511.	2.1	38

WEIQING ZHENG

#	Article	IF	CITATIONS
19	Modulating the dynamics of BrÃ,nsted acid sites on PtWOx inverse catalyst. Nature Catalysis, 2022, 5, 144-153.	34.4	35
20	Process Intensification for Cellulosic Biorefineries. ChemSusChem, 2017, 10, 2566-2572.	6.8	32
21	Production of high-yield short-chain oligomers from cellulose <i>via</i> selective hydrolysis in molten salt hydrates and separation. Green Chemistry, 2019, 21, 5030-5038.	9.0	32
22	Ethane Dehydrogenation on Single and Dual Centers of Ga-modified Î ³ -Al ₂ O ₃ . ACS Catalysis, 2021, 11, 1380-1391.	11.2	30
23	ZnO nanorod arrays assembled on activated carbon fibers for photocatalytic degradation: Characteristics and synergistic effects. Chemosphere, 2020, 261, 127731.	8.2	26
24	Intensified microwave-assisted heterogeneous catalytic reactors for sustainable chemical manufacturing. Chemical Engineering Journal, 2021, 420, 130476.	12.7	24
25	Production of renewable oleo-furan surfactants by cross-ketonization of biomass-derived furoic acid and fatty acids. Catalysis Science and Technology, 2021, 11, 2762-2769.	4.1	13
26	Experimental data-driven reaction network identification and uncertainty quantification of CO2-assisted ethane dehydrogenation over Ga2O3/Al2O3. Chemical Engineering Science, 2021, 237, 116534.	3.8	12
27	CO ₂ -assisted ethane oxidative dehydrogenation over MoO _{<i>x</i>} catalysts supported on reducible CeO ₂ –TiO ₂ . Catalysis Science and Technology, 2021, 11, 5791-5801.	4.1	11
28	Spectroscopic characterization of a highly selective NiCu ₃ /C hydrodeoxygenation catalyst. Catalysis Science and Technology, 2018, 8, 6100-6108.	4.1	9
29	Core–Shell Nanocatalyst Design by Combining Highâ€Throughput Experiments and Firstâ€Principles Simulations. ChemCatChem, 2013, 5, 3712-3718.	3.7	8
30	110th Anniversary: Kinetics and X-ray Absorption Spectroscopy in Methane Total Oxidation over Alumina-Supported Pt, Pd, and Ag–Pd Catalysts. Industrial & Engineering Chemistry Research, 2019, 58, 17718-17726.	3.7	8
31	Reversible Formation of Silanol Groups in Two-Dimensional Siliceous Nanomaterials under Mild Hydrothermal Conditions. Journal of Physical Chemistry C, 2020, 124, 18045-18053.	3.1	7
32	Higher loadings of Pt single atoms and clusters over reducible metal oxides: application to C–O bond activation. Catalysis Science and Technology, 2022, 12, 2920-2928.	4.1	7
33	<i>In Situ</i> Tracking of Nonthermal Plasma Etching of ZIF-8 Films. ACS Applied Materials & Interfaces, 2022, 14, 19023-19030.	8.0	7
34	Molten Salt Hydrates in the Synthesis of TiO ₂ Flakes. ACS Omega, 2019, 4, 21302-21310.	3.5	4
35	Volcano curves for homologous series reactions: Oxidation of small alkanes. Applied Catalysis A: General, 2019, 587, 117255.	4.3	2
36	Catalytic Hydrodeoxygenation of High Carbon Furylmethanes to Renewable Jet-fuel Ranged Alkanes over a Rhenium-Modified Iridium Catalyst. ChemSusChem, 2017, 10, 3164-3164.	6.8	0

#	Article	IF	CITATIONS
37	Selective Hydrodeoxygenation of Vegetable Oils and Waste Cooking Oils to Green Diesel Using a Silica-Supported Ir-ReO _{<i>x</i>} Bimetallic Catalyst. ChemSusChem, 0, , .	6.8	Ο